On a Class of Higher-Order Fully Decoupled Schemes for the Biot Model

Qi Zhang and Shuyu Sun*[0000−0002−3078−864X]

School of Mathematical Sciences, Tongji University, Shanghai 200092, China
suns@tongji.edu.cn

Abstract. In this paper, we consider a temporally high-order, decoupled, linear and fully discrete finite element method for the Biot model. The generalized BDF method and the simplified auxiliary variable method with correction are adopted to discretize the proposed Biot model in time. Compared with the existing works for classical BDF for the Biot model, which is addressed by several novel techniques. For an arbitrary time step, we analytically prove the time-discretized energy stability. Through a series numerical experiments, we verify the stability and accuracy of the proposed scheme.

Keywords: Biot model · Generalized BDF · Energy stability.

1 Introduction

The following quasi-static Biots consolidation problem read: for a given $\Omega \subset \mathbb{R}^d (d = 2, 3)$ with bounded, connected domain with Lipschitz continuous boundary, find the displacement field $\mathbf{u} : [0, T] \times \Omega \to \mathbb{R}^d$ and pressure field $p : [0, T] \times \Omega \to \mathbb{R}$ such that

$$-\nabla \cdot \boldsymbol{\sigma}(\mathbf{u}) + \alpha \nabla p = \boldsymbol{f} \qquad \text{in } \Omega \times [0, T], \tag{1}$$

$$\frac{\partial}{\partial t}\left(c_0 p + \alpha \nabla \cdot \boldsymbol{u}\right) - \nabla \cdot (\kappa \nabla p) = g \qquad \text{in } \Omega \times [0, T], \tag{2}$$

$$\mathbf{u}(\boldsymbol{x}, 0) = \mathbf{u}_0, p(\boldsymbol{x}, 0) = p_0 \qquad \text{in } \Omega,$$

$$\boldsymbol{u} = \mathbf{0}, p = 0 \qquad \text{on } \partial\Omega \times [0, T],$$

where $\boldsymbol{f} : [0, T] \times \Omega \to \mathbb{R}^d$ is the body force and $g : [0, T] \times \Omega \to \mathbb{R}$ is the volumetric source/sink term. The quantity $\boldsymbol{\sigma}(\mathbf{u}) = 2\mu\boldsymbol{\varepsilon}(\mathbf{u}) + \lambda \operatorname{tr}(\boldsymbol{\varepsilon}(\mathbf{u}))\mathbf{I}$ in (1) is the elastic stress tensor and involves the displacement $\mathbf{u}$, the linearized strain tensor $\boldsymbol{\varepsilon}(\mathbf{u}) = \frac{1}{2}(\nabla \mathbf{u} + \nabla \mathbf{u}^\top)$, the $d \times d$ identity matrix $\mathbf{I}$, and the elastic moduli $\mu = E/(2(1 + \nu))$ and $\lambda = E\nu/((1 + \nu)(1 - 2\nu))$ are the two Lamé coefficients, defined in terms of Young's modulus E and Poisson's ratio ν. Moreover, $c_0 \geq 0$ is the constrained specific storage coefficient, κ is the permeability and $\alpha > 0$ is the BiotWillis fluidsolid coupling coefficient, which is close to 1 and much smaller than the typical Lamé constants.

This paper develops higher-order, fully decoupled, linear, and unconditionally energy-stable schemes for Biots quasi-static poroelasticity model [1,2]. Existing

ICCS Camera Ready Version 2026
To cite this paper please use the final published version:
DOI: 10.1007/978-3-032-29924-6_23

finite element and decoupling methods for the Biot system [3,4] are mainly first-order accurate. To overcome the displacement–pressure coupling and parameter sensitivity, we exploit the cancellation structure in the energy law and apply the scalar auxiliary variable (SAV) approach [5]. For heterogeneous permeability, we further introduce a the explicit decomposition auxiliary variable (EDAV) strategy inspired by the corrected scalar auxiliary variable (CSAV) methods [6]. Combined with a generalized high-order backward difference formulae (BDF) framework [7] and a stabilization term, the resulting schemes are efficient, robust, and unconditionally energy stable.

The rest of the paper is organized as follows. Section 2 presents preliminary inequalities and results. Section 3 develops the fully discrete schemes and proves unconditional energy stability. Numerical experiments and conclusions are given in Sections 4 and 5, respectively.

2 Preliminaries and model's equivalent transformation

2.1 Preliminaries

As in [8], for $s \geq 0$, we denote $\|\cdot\|_s$ as the norms for the standard Sobolev spaces $H^s(\Omega)^d$. We also denote by $H_0^s(\Omega)^d$ the closure of $C_0^\infty(\Omega)^d$ with respect to the norm $\|\cdot\|_s$. In particular, $(\cdot,\cdot) := (\cdot,\cdot)_\Omega$ and $\|\cdot\|_0$ denote the inner product and norm in $L^2 := L^2(\Omega)$ or $L^2(\Omega)^d$, respectively.

As [9], we now derive the energy law at the PDE level for the Biot's includes (1)-(2).

Lemma 1. *The Biot's model (i.e., Eqs.* (1)-(2)*) satisfies the following energy law:*

$$\frac{d}{dt}E(\mathbf{u},p,\boldsymbol{f}) + \kappa\|\nabla p\|_0^2 = (g,p) - (\partial_t \boldsymbol{f},\mathbf{u}), \tag{3}$$

where $E(\mathbf{u},p,\boldsymbol{f}) := \frac{1}{2}\left[2\mu\|\boldsymbol{\epsilon}(\mathbf{u})\|_0^2 + \lambda\|\nabla\cdot\mathbf{u}\|_0^2 + c_0\|p(t)\|_0^2\right] - (\boldsymbol{f},\mathbf{u})$.

To apply energy techniques in our stability analysis, we recall the following lemma from Dahlquists G-stability theory [10].

Lemma 2. *Let* $\alpha(\zeta) = \alpha_k\zeta^k + \cdots + \alpha_0$ *and* $\mu(\zeta) = \mu_k\zeta^k + \cdots + \mu_0$ *be polynomials of degree at most* k*, with at least one of degree* k*, and assume that they have no common divisor. Let* $(\cdot,\cdot)$ *be an inner product with associated norm* $|\cdot|$*. If*

$$\operatorname{Re}\frac{\alpha(\zeta)}{\mu(\zeta)} > 0 \quad \textit{for } |\zeta| > 1, \tag{3.3}$$

then there exists a symmetric positive definite matrix $\mathbf{G} = (g_{ij}) \in \mathbb{R}^{k\times k}$ *and real numbers* $\delta_0,\ldots,\delta_k$ *such that, for any vectors* $v^0,\ldots,v^k$ *in the inner product space,*

$$\Big(\sum_{i=0}^{k}\alpha_i v^i, \sum_{j=0}^{k}\mu_j v^j\Big)^2 = \sum_{i,j=1}^{k} g_{ij}(v^i,v^j) - \sum_{i,j=1}^{k} g_{ij}(v^{i-1},v^{j-1}) + \Big|\sum_{i=0}^{k}\delta_i v^i\Big|^2. \tag{3.4}$$

ICCS Camera Ready Version 2026
To cite this paper please use the final published version:
DOI: 10.1007/978-3-032-29924-6_23

2.2 Model's equivalent transformation

Unlike the CSAV approach in [6], we account for heterogeneous permeability by partitioning $\Omega = \bigcup_{i=1}^{M} \Omega_i$ and introducing local auxiliary variables Q_i.

$$(Q_i^2)_t = 0, \quad Q_i|_{t=0} = 1. \tag{4}$$

Motivated by the fact that (4) admits the unique solution $Q_i \equiv 1$, we define the ODE system so that each Q_i remains close to 1. Consequently, $V(Q_i) \equiv 1$ on each Ω_i with $V(Q_i) = 1 - (1 - Q_i)^k$. Let $Q = (Q_1, \ldots, Q_M)^\top$. We further introduce a global quantity $\widetilde{V}(Q)$ with $\widetilde{V}(Q) \equiv 1$. Therefore, inserting $\widetilde{V}(Q)$ into the linear coupling terms does not alter the original Biot system (1)–(2), which can thus be reformulated equivalently as follow

$$-\nabla \cdot \boldsymbol{\sigma} + \alpha \widetilde{V}(Q) \nabla p = \boldsymbol{f} \qquad \text{in } \Omega \times [0,T], \tag{5}$$

$$\frac{\partial}{\partial t}\left(c_0 p + \alpha \nabla \cdot \boldsymbol{u}\right) - \nabla \cdot (\kappa \nabla p) + s_p \widetilde{V}(Q)\,(p - p) = g \qquad \text{in } \Omega \times [0,T], \tag{6}$$

$$\begin{aligned} &(Q_i^2)_t + \theta_i \left(s_p(p,p)_{\Omega_i} + \alpha(p, \nabla \cdot \mathbf{u}_t)_{\Omega_i}\right) V(Q_i) \\ &= \theta_i \left(s_p(p,p)_{\Omega_i} + \alpha(p, \nabla \cdot \mathbf{u}_t)_{\Omega_i}\right) V(Q_i) \qquad \text{in } [0,T], \end{aligned} \tag{7}$$

where θ_i is small parameter and s_p is a stabilization parameter to be determined later. The initial conditions and the boundary conditions remain unchanged. We now clarify the role of Q_i and the ODE system (7). Since the integral terms sum to zero, $Q_i(t) \equiv 1$. To improve robustness and keep Q_i close to 1, we add the term $s_p V(Q_i)(p - p, p)_{\Omega_i}$. The roles of $\widetilde{V}(Q)$ and $V(Q_i)$ will be discussed later.

3 Numerical scheme

This section presents temporal discretization methods for (5)–(7) based on generalized backward differentiation formula (BDF) techniques. The resulting schemes are flexible, efficient, linear, and unconditionally energy stable.

3.1 Scheme construction

Let $\mathcal{T}_h$ be a shape-regular mesh of Ω. The finite element spaces are

$$\mathbf{X}_h = \{\mathbf{u} \in (H_0^1(\Omega))^d : \mathbf{u}|_K \in \mathcal{P}_{\ell_1}(K)\}, \quad M_h = \{p \in H_0^1(\Omega) : p|_K \in \mathcal{P}_{\ell_2}(K)\}.$$

For the temporal discretization, we use the generalized BDF-k method ($2 \le k \le 3$) together with a kth-order extrapolation. Let $t^n = n\Delta t$. Then

$$\frac{1}{\Delta t} \sum_{q=0}^{k} a_{k,q}(\beta) \phi(t^{n+1-k+q}) = \partial_t \phi(t^{n+\beta}) + \mathcal{O}(\Delta t^k), \tag{8}$$

$$\sum_{q=0}^{k-1} b_{k,q}(\beta) \phi(t^{n+2-k+q}) = \phi(t^{n+\beta}) + \mathcal{O}(\Delta t^k), \tag{9}$$

ICCS Camera Ready Version 2026
To cite this paper please use the final published version:
DOI: 10.1007/978-3-032-29924-6_23

$$\sum_{q=0}^{k-1} c_{k,q}(\beta)\phi(t^{n+1-k+q}) = \phi(t^{n+\beta}) + \mathcal{O}(\Delta t^k). \tag{10}$$

Remark 1. For convenience, the coefficients in (8)–(10) for $k = 2, 3$ are listed below; see [7] for details.

For convenience, we introduce

$$A_k^\beta(\phi^{n+1}) = \sum_{q=0}^{k} a_{k,q}(\beta)\phi^{n+1-k+q},\ B_k^\beta(\phi^{n+1}) = \sum_{q=0}^{k-1} b_{k,q}(\beta)\phi^{n+2-k+q}, \tag{11}$$

$$C_k^\beta(\phi^n) = \sum_{q=0}^{k-1} c_{k,q}(\beta)\phi^{n+1-k+q},\ B_k^\beta(\phi^{n+1}) = \eta_k(\beta)C_k^\beta(\phi^{n+1}) + D_k^\beta(\phi^{n+1}),$$

where $\eta_2(\beta) = \frac{\beta-1}{\beta}$, $\eta_3(\beta) = \frac{\beta-1}{\beta+1}$, $\beta \geq 1$, and

$$d_{k,q}(\beta) = b_{k,q}(\beta) - \eta_k(\beta)c_{k,q}(\beta), \qquad D_k^\beta(\phi^{n+1}) = \sum_{q=0}^{k-1} d_{k,q}(\beta)\phi^{n+2-k+q}. \tag{12}$$

The numerical scheme of system (5)-(7) is formulated as follows:

Algorithm 3.1 EDAV-GBDF scheme

Step 1: Find $\mathbf{u}_h^{n+1} \in \mathbf{X}_h$ such that for all $\mathbf{v}_h \in \mathbf{X}_h$

$$\begin{aligned} &2\mu\left(\boldsymbol{\epsilon}(B_k^{\beta_k+1}(\mathbf{u}_h^{n+1})), \boldsymbol{\epsilon}(\mathbf{v}_h)\right) + \lambda\left(\nabla\cdot B_k^{\beta_k+1}(\mathbf{u}_h^{n+1}), \nabla\cdot\mathbf{v}_h\right) \\ &-\left(\alpha\widetilde{V}(Q^n)C_k^{\beta_k+1}(p_h^n), \nabla\cdot\mathbf{v}_h\right) = \left(\boldsymbol{f}^{n+\beta_k+1}, \mathbf{v}_h\right), \end{aligned} \tag{13}$$

Step 2: Find p_h^{n+1} such that for all $q_h \in M_h$

$$\begin{aligned} &c_0\left(\frac{A_k^{\beta_k}(p_h^{n+1})}{\Delta t}, q_h\right) + \alpha\left(\widetilde{V}(Q^n)\nabla\cdot\left(\frac{A_k^{\beta_k}(\mathbf{u}_h^{n+1})}{\Delta t}\right), q_h\right) + \left(\kappa\nabla B_k^{\beta_k}(p^{n+1}), \nabla q_h\right) \\ &+ s_p\widetilde{V}(Q^n)\left(B_k^\beta(p_h^{n+1}) - C_k^\beta(p_h^n), q_h\right) = \left(g^{n+\beta_k}, q_h\right). \end{aligned} \tag{14}$$

Step 3: Find $\widetilde{Q}_i^{n+1} \in \mathbb{R}$ such that

$$\begin{aligned} \frac{(\widetilde{Q}_i^{n+1})^2 - (Q_i^n)^2}{\Delta t} =& \theta_i\alpha V(Q_i^n)\left(C_k^{\beta_k}(p^{n+1}) - C_k^{\beta_k+1}(p_h^n), \nabla\cdot\frac{A_k^{\beta_k}(\mathbf{u}_h^{n+1})}{\Delta t}\right)_{\Omega_i} \\ &+ \theta_i s_p\widetilde{V}(Q^n)\left(B_k^\beta(p_h^{n+1}) - C_k^\beta(p_h^n), C_k^{\beta_k}(p^{n+1})\right)_{\Omega_i}. \end{aligned} \tag{15}$$

Step 4: To improve consistency, we further implement the following correction $\left(Q_i^{n+1}\right)^2 = \xi\left(\widetilde{Q}_i^{n+1}\right)^2 + (1-\xi)$, where $\xi \in [0,1]$ such that

$$\left(Q_i^{n+1}\right)^2 - \left(\widetilde{Q}_i^{n+1}\right)^2 \leq \Im\mathcal{R}_i^{n+1}, \quad 0 < \Im < 1. \tag{16}$$

ICCS Camera Ready Version 2026
To cite this paper please use the final published version:
DOI: 10.1007/978-3-032-29924-6_23

with $\mathcal{R}_i^{n+1} = \frac{3\eta_k}{4}\kappa\Delta t\|\nabla C_k^\beta(p_h^{n+1})\|_{0,\Omega_i}^2$, $k = 2, 3$ We choose an appropriate ξ according to the following four cases:

- If $\widetilde{Q}_i^{n+1} = 1$, we set $\xi = 0$;
- If $\widetilde{Q}_i^{n+1} > 1$, we set $\xi = 0$;
- If $\widetilde{Q}_i^{n+1} < 1$ and $\left(\widetilde{Q}_i^{n+1}\right)^2 + \Im\mathcal{R}_i^{n+1} \geq 1$, we set $\xi = 0$;
- If $\widetilde{Q}_i^{n+1} < 1$ and $\left(\widetilde{Q}_i^{n+1}\right)^2 + \Im\mathcal{R}_i^{n+1} < 1$, we set $\xi = 1 - \frac{\Im\mathcal{R}_i^{n+1}}{1-\widetilde{Q}_i^{n+1}}$.

So, Q^{n+1} can be shown to be expressed as $Q^{n+1} = Q_i^{n+1}$ in Ω_i and $\widetilde{V}(Q^{n+1}) = V(Q_i^{n+1})$ in Ω_i.

Theorem 1. *By Lemma 1 and Theorem 1 in [7], in the absence of the external force $\boldsymbol{f}$, and with the first $k-1$ steps generated by a coupling scheme. Let λ_k^g be the smallest eigenvalue of the matrix $\mathbf{G}$, the EDAV-GBDF scheme with $k = 2, 3$ and $\beta > 1$ is unconditionally stable in the sense that*

$$
\begin{aligned}
&2\mu\lambda_k^g\|\boldsymbol{\epsilon}(\mathbf{u}^N)\|_0^2 + \lambda\lambda_k^g\|\nabla\cdot\mathbf{u}^{N+i-k}\|_0^2 + c_0\lambda_k^g\|p^{n+1+i-k}\|_0^2 \\
&\quad + \frac{3\,(1-\Im)\,\kappa}{4}\eta_k\Delta t\sum_{k-1}^{N-1}\|\nabla C_k^\beta(p_h^{n+1})\|_0^2 + \kappa\hat{\lambda}_k^h\Delta t\|\nabla p^N\|_0 + \sum_{i=1}^{M}\frac{(Q_i^N)^2}{\theta_i} \\
&\leq C\Bigg(2\mu\sum_{i=1}^{k}\|\boldsymbol{\epsilon}(\mathbf{u}^{i-1})\|_0^2 + \lambda C\sum_{i=1}^{k}\|\nabla\cdot\mathbf{u}^{i-1}\|_0^2 + c_0 C\sum_{i=1}^{k}\|p^{i-1}\|_0^2 \\
&\quad + \kappa C\Delta t\sum_{i}^{k}\|\nabla p^{i-1}\|_0^2\Bigg) + \sum_{i=1}^{M}\frac{(Q_i^{k-1})^2}{\theta_i}. \qquad (17)
\end{aligned}
$$

Proof. Taking $\mathbf{v}_h = A_k^\beta(\mathbf{u}_h^{n+1})$ in (13) and $q_h = \Delta t\, C_k^\beta(p_h^{n+1})$ in (14), and then combining the resulting equations, we obtain, by Lemma 1, Theorem 1 in [7], and (11), that

$$
\begin{aligned}
&2\mu\sum_{i,j=1}^{k} g_{ij}\left(\boldsymbol{\epsilon}(\mathbf{u}^{n+1+i-k}), \boldsymbol{\epsilon}(\mathbf{u}^{n+1+j-k})\right) - 2\mu\sum_{i,j=1}^{k} g_{ij}\left(\boldsymbol{\epsilon}(\mathbf{u}^{n+i-k}), \boldsymbol{\epsilon}(\mathbf{u}^{n+j-k})\right) \\
&+ \lambda\sum_{i,j=1}^{k} g_{ij}\left(\nabla\cdot\mathbf{u}^{n+1+i-k}, \nabla\cdot\mathbf{u}^{n+1+j-k}\right) - \lambda\sum_{i,j=1}^{k} g_{ij}\left(\nabla\cdot\mathbf{u}^{n+i-k}, \nabla\cdot\mathbf{u}^{n+j-k}\right) \\
&+ c_0\sum_{i,j=1}^{k} g_{ij}\left(p^{n+1+i-k}, p^{n+1+j-k}\right) - c_0\sum_{i,j=1}^{k} g_{ij}\left(p^{n+i-k}, p^{n+j-k}\right) \\
&+ \kappa\Delta t\sum_{i,j=1}^{k} h_{ij}\left(\nabla p^{n+1+i-k}, \nabla p^{n+1+j-k}\right) - \kappa\Delta t\sum_{i,j=1}^{k} h_{ij}\left(\nabla p^{n+i-k}, \nabla p^{n+j-k}\right) \\
&+ \alpha\widetilde{V}(Q^n)\left(\nabla\cdot A_k^\beta(\mathbf{u}_h^{n+1}), C_k^\beta(p_h^{n+1})\right) - \alpha\widetilde{V}(Q^n)\left(C_k^{\beta+1}(p_h^n), \nabla\cdot A_k^\beta(\mathbf{u}_h^{n+1})\right) \\
&+ s_p\widetilde{V}(Q^n)\Delta t\left(B_k^\beta(p_h^{n+1}) - C_k^\beta(p_h^n), C_k^\beta(p_h^{n+1})\right) + \eta_k\kappa\Delta t\|\nabla C_k^\beta(p_h^{n+1})\|_0^2
\end{aligned}
$$

ICCS Camera Ready Version 2026
To cite this paper please use the final published version:
DOI: 10.1007/978-3-032-29924-6_23

$$\leq \frac{C_p}{\eta_k}\Delta t\|g^{n+\beta}\|_0 + \frac{\eta_k\kappa}{4}\Delta t\|\nabla C_k^{\beta}(p_h^{n+1})\|_0^2 \tag{18}$$

Then, using (15), (16) and (18), and summing (18) form $k-1=1$ to $N-1$, we get

$$\begin{aligned}
&2\mu\lambda_k^g\|\boldsymbol{\epsilon}(\mathbf{u}^N)\|_0^2 + \lambda\lambda_k^g\|\nabla\cdot\mathbf{u}^{N+i-k}\|_0^2 + c_0\lambda_k^g\|p^{n+1+i-k}\|_0^2 \\
&\quad + \frac{3\eta_k\kappa}{4}\Delta t\sum_{k-1}^{N-1}\|\nabla C_k^{\beta}(p_h^{n+1})\|_0^2 + \kappa\hat{\lambda}_k^h\Delta t\|\nabla p^N\|_0 + \sum_{i=1}^{M}\frac{(Q_i^N)^2}{\theta_i} \\
&\leq 2\mu\sum_{i,j=1}^{k} g_{ij}\left(\boldsymbol{\epsilon}(\mathbf{u}^{i-1}),\boldsymbol{\epsilon}(\mathbf{u}^{j-1})\right) + \lambda\sum_{i,j=1}^{k} g_{ij}\left(\nabla\cdot\mathbf{u}^{i-1},\nabla\cdot\mathbf{u}^{j-1}\right) \\
&\quad + c_0\sum_{i,j=1}^{k} g_{ij}\left(p^{i-1},p^{j-1}\right) + \kappa\Delta t\sum_{i,j=1}^{k} h_{ij}\left(\nabla p^{i-1},\nabla p^{j-1}\right) + \sum_{i=1}^{M}\frac{(Q_i^{k-1})^2}{\theta_i}.
\end{aligned} \tag{19}$$

Hence, using the above estimate, Hölder and Youngs inequalities, we obtain (17). The proof is completed.

4 Numerical experiments

Example 1. Convergence test. In this test, we take the computational domain to be the unit square and choose the source term, boundary conditions, and initial data so that the exact solution of (1)–(2) is

$$\begin{aligned}
u_1(x,y,t) &= e^{-t}\left(\sin(2\pi y)(-1+\cos(2\pi x)) + \frac{1}{\mu+\lambda}\sin(\pi x)\sin(\pi y)\right), \\
u_2(x,y,t) &= e^{-t}\left(\sin(2\pi x)(1-\cos(2\pi y)) + \frac{1}{\mu+\lambda}\sin(\pi x)\sin(\pi y)\right), \\
p(x,y,t) &= e^{-t}\sin(\pi x)\sin(\pi y).
\end{aligned}$$

We set $\ell_1 = 3$, $\ell_2 = 2$ and $h = 1/150$ so that the spatial error is negligible. In this example, we choose $\theta = 10^{-4}, c_0 = 10^{-8}$, $\kappa = 1$, $\mu = 1$, $\lambda = 1$, $\alpha = 1$. Tables 1 confirm the expected convergence orders for $k = 3$. Here $\Delta t_{\text{init}} = 10^{-8}$ is chosen so that the initialization error is negligible. The results confirm the predicted spatial convergence rates.

Table 1: Errors and convergent rates of 2D with $k = 3, \beta = 6$ and $s_p = 10$.

Δt	$\|\mathbf{e}_u\|_0$	Rate	$\|\nabla\mathbf{e}_u\|_0$	Rate	$\|e_p\|_0$	Rate	$\|\nabla e_p\|_0$	Rate
$\frac{1}{8}$	3.1173e-02	-	2.2078e-01	-	6.0911e-03	-	2.7855e-02	-
$\frac{1}{16}$	8.7438e-03	1.83	6.1900e-02	1.83	1.4996e-03	2.02	6.6766e-03	2.06
$\frac{1}{32}$	9.7624e-04	3.16	6.9100e-03	3.16	1.4921e-04	3.33	6.6472e-04	3.33
$\frac{1}{64}$	1.0878e-04	3.16	7.6997e-04	3.16	1.7836e-05	3.06	8.6792e-05	2.94

ICCS Camera Ready Version 2026
To cite this paper please use the final published version:
DOI: 10.1007/978-3-032-29924-6_23

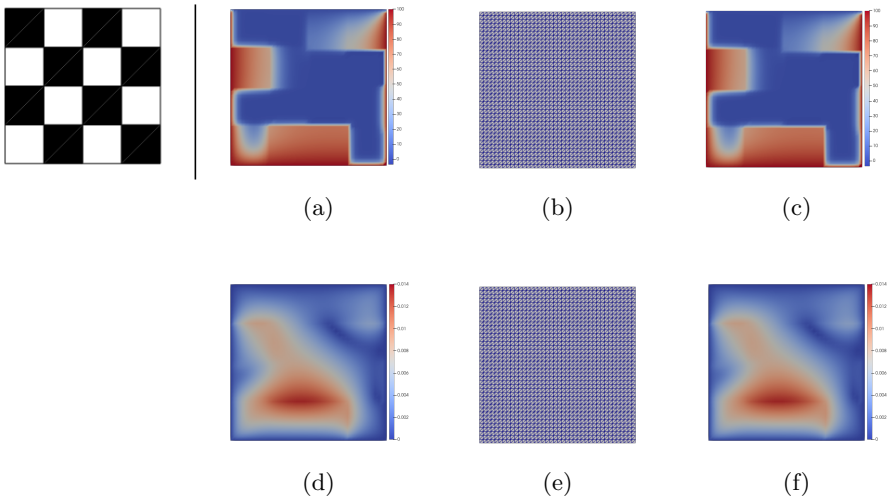

Fig. 1: Configurations of heterogeneous material properties. Panels (a)–(c) show the pressure computed by the coupling algorithm, the monolithic method, and the domain decomposition method, respectively. Panels (d)–(f) show the corresponding displacement magnitude, $|\mathbf{u}|$.

Example 2. Heterogeneous coefficients. Following [11], we consider (1)–(2) on $\Omega = (0,1)^2$ with discontinuous, piecewise constant coefficients on a 4×4 partition; see Figure 1. And the boundary segments are ordered as bottom, right, top, and left. We take

$$\boldsymbol{f} = \left(\tfrac{1}{2}(1-\cos(2\pi t)), 0\right)^T, \ g = 0, \ \mathbf{u} = \mathbf{0} \quad \text{on } \partial\Omega \times (0,T].$$

with boundary conditions $\nabla p \cdot \boldsymbol{n} = 0$ on $\Gamma_3 \times (0,T]$, $p = 1$ on $\Gamma_j \times (0,T]$, $j = 1,2,4$. The parameters are set to $c_0 = 1$, $\mu = 10$, $\lambda = 10^3$, $\alpha = 1$, while the permeability κ is prescribed piecewise by

$$\kappa = \begin{bmatrix} 10^{-2} & 10^{-1} & 10^{-1} & 10^{-6} \\ 10^{-3} & 10^{-5} & 10^{-4} & 10^{-3} \\ 10^{-1} & 10^{-2} & 10^{-5} & 10^{-4} \\ 10^{-6} & 10^{-3} & 10^{-1} & 1 \end{bmatrix}.$$

For both the coupled and the EDAV-GBDF algorithms with $k = 2$, we set $h = 1/40$, $\Delta t = 0.05$, $\Delta t_{\text{init}} = 10^{-8}$, and $T = 0.5 + 10^{-8}$. For the EDAV-GBDF algorithm, we use $\beta = 2$, $s_p = 10^{-6}$, and $\theta_i = 0.5$, and compare regional partitioning ($M = 16$) with holistic treatment ($M = 1$) of the auxiliary variables. Figure 1 shows that regional partitioning gives more accurate results and performs comparably to the coupled algorithm, whereas the holistic treatment is less effective.

ICCS Camera Ready Version 2026
To cite this paper please use the final published version:
DOI: 10.1007/978-3-032-29924-6_23

5 Conclusion

In summary, we propose a high-order finite element time-stepping scheme for the Biot model that is linear and fully decoupled. The scheme is unconditionally energy stable, and numerical results confirm the expected accuracy and robustness.

Acknowledgments. The authors gratefully acknowledge the financial support from the National Key Research and Development Project of China (Grant No. 2023YFA1011701), the National Natural Science Foundation of China (Grant No. 12571466), and the Fundamental Research Funds for the Central Universities. In addition, Shuyu Sun would like to express his gratitude for the support provided by the Shanghai Magnolia Talent Fund (Innovation Talent Category) of Shanghai Municipal Human Resources and Social Security Bureau and the Chang Jiang Scholars Program of the Ministry of Education of China.

Disclosure of Interests. The authors have no competing interests to declare that are relevant to the content of this article.

References

1. Terzaghi, K.: Theoretical soil mechanics. Wiley, New York (1943)
2. Biot, M.A.: Theory of elasticity and consolidation for a porous anisotropic solid. Journal of Applied Physics **26**(2), 182–185 (1955)
3. Yi, S.-Y.: A study of two modes of locking in poroelasticity. SIAM Journal on Numerical Analysis **55**(4), 1915–1936 (2017)
4. Altmann, R., Maier, R., Unger, B.: Semi-explicit discretization schemes for weakly coupled elliptic-parabolic problems. Mathematics of Computation **90**(329), 1089–1118 (2021)
5. Shen, J., Xu, J., Yang, J.: The scalar auxiliary variable (SAV) approach for gradient flows. Journal of Computational Physics **353**, 407–416 (2018)
6. Yang, J., Kim, J.: On a two-phase incompressible diffuse interface fluid model with curvature-dependent mobility. Journal of Computational Physics **525**, 113764 (2025)
7. Huang, F., Shen, J.: On a new class of BDF and IMEX schemes for parabolic type equations. SIAM Journal on Numerical Analysis **62**(4), 1609–1637 (2024)
8. Temam, R.: Navier–Stokes Equations: Theory and Numerical Analysis. AMS Chelsea Publishing, Providence (1984)
9. Zhao, J., Chen, H., Sun, S., Li, H.: Unconditionally energy-stable and locking-free parallel splitting finite element method for the Biot model. Journal of Scientific Computing **104**(3), 74 (2025)
10. Dahlquist, G.: G-stability is equivalent to A-stability. BIT Numerical Mathematics **18**(4), 384–401 (1978)
11. Cai, M., Pavarino, L.F., Widlund, O.B.: Overlapping Schwarz methods with a standard coarse space for almost incompressible linear elasticity. SIAM Journal on Scientific Computing **37**(2), A811–A830 (2015)

ICCS Camera Ready Version 2026
To cite this paper please use the final published version:
DOI: 10.1007/978-3-032-29924-6_23